

# Characterization of the electrical properties of an optical device manufactured with CMOS 0.35 $\mu\text{m}$ technology

Ricardo Yauri<sup>1,2</sup>, Vanessa Gamero<sup>3</sup>, Marco Alayo<sup>3</sup>

<sup>1</sup>Facultad de Ingeniería, Universidad Tecnológica del Perú, Lima, Perú

<sup>2</sup>Facultad de Ingeniería Electrónica y Eléctrica, Universidad Nacional Mayor de San Marcos, Lima, Perú

<sup>3</sup>Departamento de Engenharia de Sistemas Eletrônicos, Universidade de São Paulo, São Paulo, Brasil

## Article Info

### Article history:

Received Mar 27, 2023

Revised Aug 19, 2023

Accepted Sep 5, 2023

### Keywords:

CMOS optical devices  
Electrical characterization  
Incandescent optical source  
Integrated optics  
Monolithic integration

## ABSTRACT

Currently, the relevance of optical devices has increased due to the physical limitations of the electrical transmission medium and the proximity of the limit of Moore's Law. Furthermore, the fabrication of optical devices on monolithic silicon substrates has gained importance in recent years thanks to manufacturing technologies in the microelectronics industry. For this reason, this paper aims to carry out the electrical characterization of an optical device manufactured with commercial austria micro system technology of complementary metal oxide semiconductors of 0.35  $\mu\text{m}$ . The methodology consists of implementing an optical device, with an incandescent optical source called a microlamp, a waveguide and a photodiode. The microlamp was projected between two metal layers connected by tungsten vias that act as filaments covered by SiO<sub>2</sub> dielectric to prevent oxidation. The results of the electrical characterization of the optical device show that the microlamp reaches a maximum current of 48 mA and stops working at higher currents. The waveguide was designed with a SiO<sub>2</sub> core and it was discovered that the TiN layers were found to be part of the waveguide causing it to behave as an emitter in the 2.5-5  $\mu\text{m}$  region.

*This is an open access article under the [CC BY-SA](https://creativecommons.org/licenses/by-sa/4.0/) license.*



## Corresponding Author:

Ricardo Yauri

Facultad de Ingeniería, Universidad Tecnológica del Perú

125 Natalio Sanchez Road, Santa Beatriz, Lima, Perú

Email: boncer99@gmail.com

## 1. INTRODUCTION

Optical devices became relevant three decades ago [1], [2], some reasons for this could be the proximity of the limit of moore's law [3] and the physical limitations of the electrical transmission medium [4]. Nowadays, the literature reports that the optical medium has greater bandwidth than the electrical medium, absence of the Joule effect and it is electromagnetic interference-free [5], [6]. Optical devices can be fabricated with standard microelectronic processes in a heterogeneous or monolithic substrate [7], [8].

The main difference of using a monolithic or heterogeneous substrate in the optical device's fabrication is that a monolithic substrate means a less complex fabrication process and opens the possibility to achieve a high packing density at lower cost. In the recent years, fabrication of optical devices in Silicon monolithic substrate have gained relevance by using well-known manufacturing technologies such as bulk-complementary metal oxide semiconductor (CMOS) and silicon-on-insulator (SOI-CMOS) [9], [10]. Silicon has some limitations for the fabrication of optical devices [11], [12] but it is still a viable option considering the plethora of techniques and processes developed in the microelectronics industry that could be used for fabrication of optical devices in many applications [10], [13], [14].

The contribution of this paper is the report of the electrical characterization of an optical device fabricated in the standard CMOS 0.35  $\mu\text{m}$  technology provided by the austria micro systems (AMS) [9], [15], [16]. The optical device has three components: a source light, that is a microlamp emulating an incandescent lamp, coupled to an optical waveguide, to guide light to device's ending that is an embedded detector, based on a PN photodiode, further description of the optical device is in [17], [18]. This paper is structured as follows: section 2, explain the concepts behind the elements of the optical device, its layout and parts and its fabrication in AMS 0.35  $\mu\text{m}$  [9], [15], [16]. Section 3 describes the optical device's characterization. Section 4 shows the results of the electrical characterization and Section 5 has the conclusions.

## 2. OPTICAL DEVICE FUNDAMENTALS

The optical device was fabricated in the back end of line (BEOL) section of the AMS CMOS 0.35  $\mu\text{m}$ . This technology has four main metal layers: Metal1 (M1), Metal2 (M2), Metal3 (M3) and Metal4 (M4). The average thickness of the metal layers is 600 nm, except for the layer M4 with thickness of 2800 nm. The interconnection between the layers is through tungsten metallic vias and the isolation between layers is with  $\text{SiO}_2$  dielectric material with thickness of 1,000 nm [19]. The optical device has three components: 1) a source light, called microlamp because it emulates an incandescent lamp; 2) a waveguide, released in the post-processing phase [17] and a photodiode for measuring the incoming light from the microlamp. The logical blocks of the optical device and the connection between them are illustrated in Figure 1.

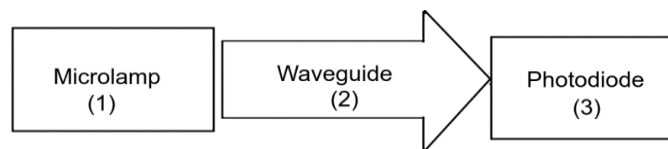


Figure 1. Components of the optical device; (1) microlamp, (2) waveguide, and (3) photodiode

### 2.1. Components of the optical device

#### 2.1.1. Microlamp

The microlamp acts as an incandescent lamp and the stages of Principle of operation and Components of the micro lamp are show in Figure 2. This has a metal filament surrounded by an insulating material as illustrated in Figure 2(a). When an electric current ( $I$ ) is injected through the microlamp filament ( $R$ ) it dissipates thermal energy that propagates as electromagnetic waves at different wavelengths [20]. This kind of light source can be found in many sensing applications because it has fast thermal response [21], [22], efficient energy consumption [23] and compatibility with commercial manufacturing processes [24].

The fabrication of the microlamp with CMOS 0.35  $\mu\text{m}$  has filaments made of tungsten vias that interconnects the metallic layers M2 and M3 and insulating material of the  $\text{SiO}_2$  dielectric placed between the metallic layers. The layers M1 and M4 (below and above the microlamp) were projected as sacrificial layers and were etched in the optical device's post-processing to prevent conductive heat loss to the metallic layers or the substrate as illustrated in Figure 2(b).

#### 2.1.2. Waveguide

An optical waveguide is a device used to confine light in a controlled manner, consisting of a core where the light is confined, cladding layers that are the waveguide's walls. The waveguide is based on Total internal reflection (RIT), where the light beams propagate through the core reflecting off the walls [25]. The waveguide was fabricated in the BEOL section and coupled to the microlamp by its core. Since the microlamp insulating material is  $\text{SiO}_2$ , the waveguide's core was also made of this material to allow the maximum transference of optical power between them. The waveguide's claddings refraction index must be lower than the core material ( $n(\text{SiO}_2)=1.46$ ), a practical solution for the claddings was air material ( $n=1$ ).

#### 2.1.3. Photodiode

The photodiode is a semiconductor device that transforms optical energy into electrical current and is made of p-type (hole-rich), n-type (electron-rich) semiconductors regions and metal contacts at the p-n junction, when these regions are in contact, there is a diffusion of electrons from the n region to the p region. The photodiode's optical device was fabricated in the front end of Line section of the CMOS 0.35  $\mu\text{m}$ , it is the PHDNWA850 (N-well and P-substrate) a ready model taken from the AMS toolkit. The photodiode responsivity characteristics and other features can be found in [26].

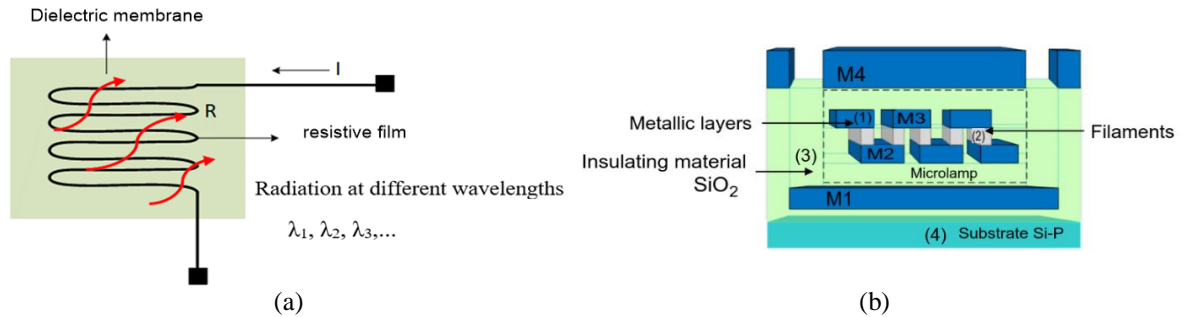


Figure 2. Description of the microlamp based on (a) working principle and (b) components

**2.2. Device components integration**

Figure 3 shows different views of the optical device with integration of the microlamp. A lateral view of device’s components integration is shown in Figure 3(a). The formation of the waveguide’s air claddings was planned with a SiO<sub>2</sub> etching of the waveguide laterals. Since the microlamp was fabricated in layers M2 and M3 and isolated from the exterior with the SiO<sub>2</sub> dielectric, it must be protected during the waveguide’s lateral etching with reactive ion etching (RIE). For this reason, the top metal layer M4 was used as an etching mask because. The layer M1 under the microlamp was also etched to isolate the microlamp from the Silicon substrate and thus avoid heat dissipation and the waveguide’s core light being absorbed by the M1 layer. It is expected that part of the light travelling in the core will make several reflections in the core to hit the photodiode, which is placed into optical device substrate. A top view of the device fabricated in CMOS 0.35 μm is shown in Figure 3(b).

After the optical device post-processing, the microlamp isolation from substrate and the waveguide air claddings formation was confirmed with the barrier electron microscope (MEV) [27] equipment JCM 600 tests facilitated from the materials processing and characterization laboratory (LPCM) of FATEC-SP. In Figure 3(c) and Figure 3(d), the optical device MEV is focusing on the microlamp and the waveguide laterals. It can be observed the microlamp suspension and air waveguide claddings.

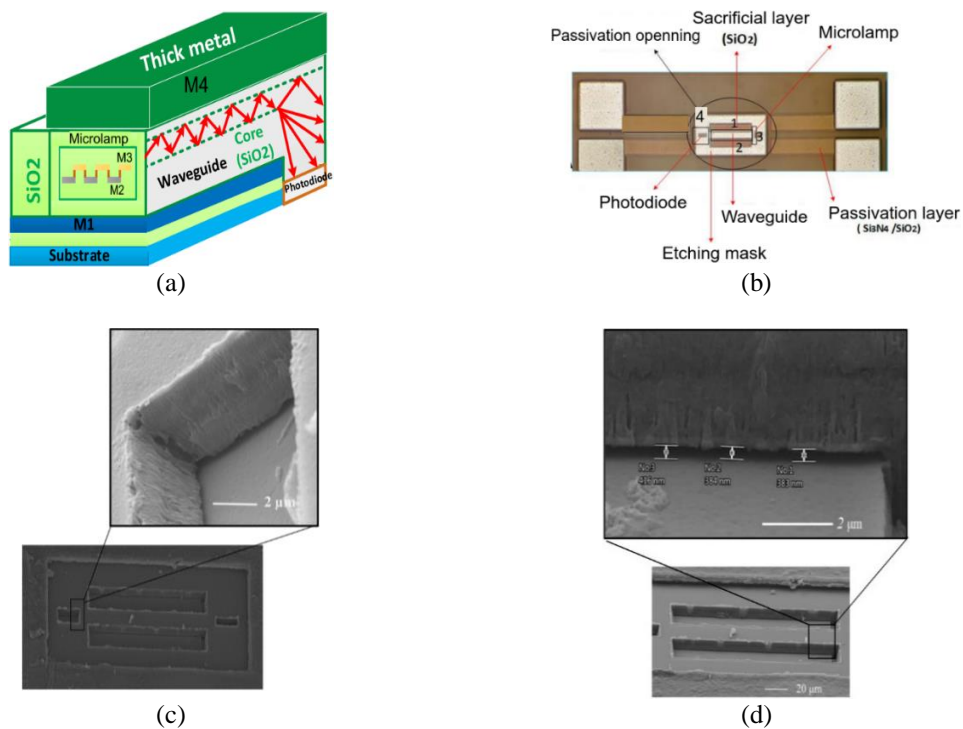


Figure 3. Visualization of the optical device using a; (a) lateral view diagram with integration of the microlamp, waveguide and photodiode, (b) frontal view of the device fabricated with CMOS 0.35 μm, (c) device MEV focusing on the microlamp region, and (d) device MEV focusing on the waveguide laterals

**3. ELECTRICAL DEVICE CHARACTERIZATION**

The electrical characterization of the optical device was carried out in two stages: first, individually in the microlamp and, second, at the junction between the waveguide and the photodiode. To perform these tests, the device was fixed on the platform of the Cascade Microtech Newport MPS150 test station, which has an anti-vibration platform and an optical microscope with a maximum capacity of 5 μm. This configuration provided the necessary conditions to carry out electrical measurements accurately.

**3.1. Microlamp characterization**

The I-V curves of the microlamp were obtained before and after the SiO<sub>2</sub> etching through a characterization process as seen in Figure 4. The microlamp resistance value was projected in 6 Ω minimizing the resistance of pad-microlamp path by placing multiple vias as shown in Figure 4(a). Some factors to be considered in the electrical characterization, is the non-desired etching of some parts in the optical device. In Figure 4(b) can be observed the path microlamp-pads attacked after the SiO<sub>2</sub> etching and scratches in the pads with the MPS150 tips observed in Figure 4(b). All these factors in conjunction could increment the final measure of the microlamp’s resistance.

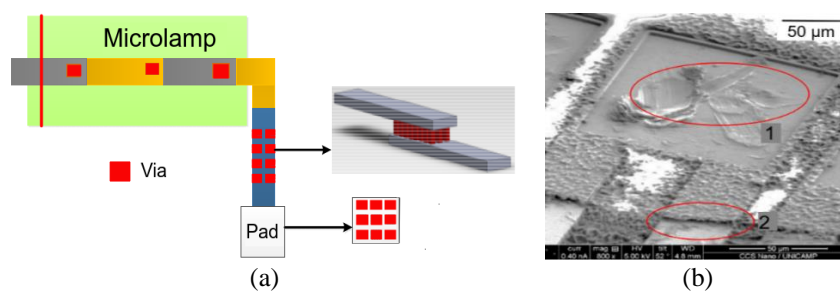


Figure 4. Microlamp characterization (a) projected resistance of the microlamp minimizing pad-microlamp path placing multiple vias and (b) microlamp after the SiO<sub>2</sub> etching

**3.2. Waveguide-photodiode characterization**

The characterization of the waveguide and photodiode was carried on using an external source light, a dichroic light with power dimerization in 25 W, 50 W e 75 W placed away 4 cm from the photodiode. The energy travelling through the waveguide could be measured by the photodiode. Considering the temperature reached by the microlamp is in the range of 181.56-230.11 °C and based on an approximation of the blackbody model, the energy radiated at these temperatures is in the mid-infrared region (2,500-5,000 nm) as it is shown in Figure 5.

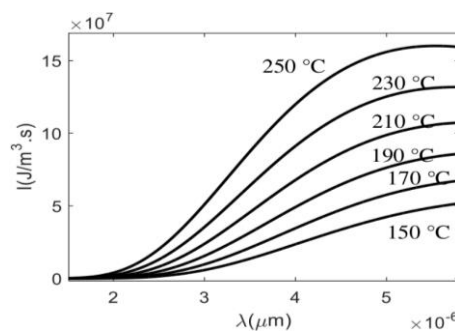


Figure 5. Energy radiated from a blackbody. Temperatures between 150-250 °C irradiates in the 0.9-1.4 μm wavelength region

**4. RESULTS OF THE ELECTRICAL CHARACTERIZATION**

**4.1. Microlamp**

The process of Characterizing the current response of the microlamps was conducted Figure 6. In a first case, the I-V curves of six microlamps were obtained using the HP 4145 semiconductor analyzer with a voltage sweep (V) of 0-0.15 V on the microlamp and current (I) limitation to 300 □A to avoid heating the

filaments. The resistances were between 33-40  $\Omega$  as observed in Figure 6(a), these values were much higher than the projected value. To obtain the maximum current (I) reached by the microlamp, a voltage sweep (V) of 0 - 3.5 V was applied in the three microlamps. The I-V curves are shown in Figure 6(b), from it is observed that the maximum current reached by the microlamps is between 47- 48.19 mA then it drops below 5 mA, indicating that the microlamp is not working anymore.

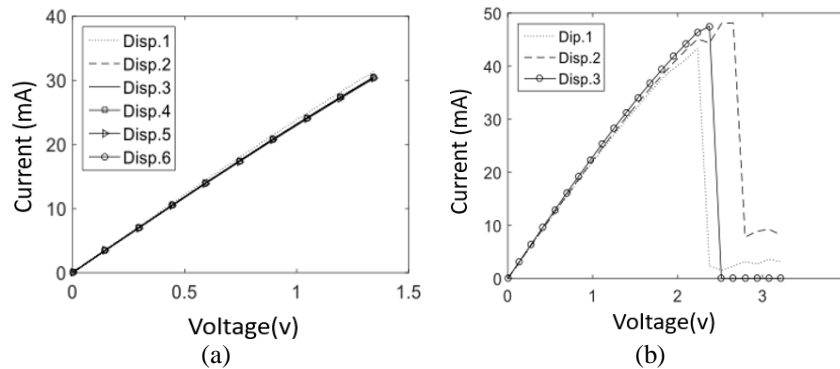


Figure 6. Characterization of the current response of (a) six microlamp responses in voltage sweep 0-1.5 V limiting current to 300  $\mu$ A and (b) maximum current values in three microlamps in voltage sweep 0-3.5V

#### 4.2. Waveguide-photodiode

The characterization of the PHDNWA850 photodiode was conducted using an external optical source and a dichroic lamp with adjustable power (25W, 50W, and 75W) placed 4 cm away from the photodiode. The I-V curve of the photodiode is shown in Figure 7. When applying a forward bias in the photodiode, the threshold voltage is approximately 0.89 V and without a light injection (0W) the current ( $I_s$ ) is approximately 400  $\mu$ A.

The CMOS 0.35  $\mu$ m AMS technology place internal titanium nitride (TiN) layers between the waveguide layers. This was observed only after a focused ion beam (FIB) on the waveguide's cross section executed the Centro de Componentes Semicondutores e Nanotecnologias (CCSNano) da Universidade Estadual de Campinas. The FIB optical device is shown in Figure 8, it can be observed that the TiN layers thickness are between 440-450 nm.

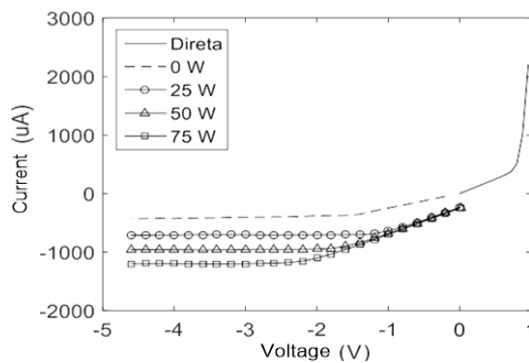


Figure 7. I-V curve of the PHDNWA850 photodiode at 0W, 25W, 50W, and 75W of power light

The microlamp's radiation region is 2.5-5  $\mu$ m based on the black body model, therefore the photodiode fabricated with silicon could not be able to detect the infrared region. Additionally, the waveguide will have other behavior because of the TiN have a higher refraction index than SiO<sub>2</sub> in the region of 2.5-5  $\mu$ m. Therefore, part of energy that strikes on the interface TiN/ SiO<sub>2</sub> will be confined in the TiN layers [28]. Finally, the photodiode could only detect up to 1,1  $\mu$ m region.

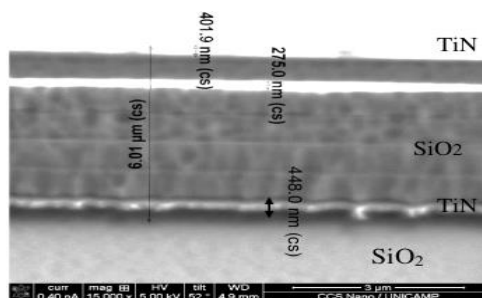


Figure 8. FIB image of the device waveguide's cross section. The thickness layers of TiN are between 400-450 nm

## 5. CONCLUSIONS

This article shows the electrical characterization process of an optical device that integrates a microlamp, a waveguide and a photodiode. fabricated with  $0.35\ \mu\text{m}$  CMOS technology from the AMS foundry. In the electrical characterization of the microlamp, it was found that the optical device withstanding maximum currents of 48.19 mA. Based on the blackbody model, the microlamp emits energy in infrared region of  $2.5\text{-}5\ \mu\text{m}$ . Therefore, it can be concluded that the microlamp could be used as an optical source (in the mid-infrared region). The waveguide was designed with a  $\text{SiO}_2$  core and air cladding, however, after FIB tests were found that TiN layers were part of the waveguide. Therefore, it can be concluded that the waveguide structure will not behave as a waveguide but as an emitter in the region of  $2.5\text{-}5\ \mu\text{m}$  because TiN is a material with high absorption in this range. Finally, the photodiode of the optical device made of Si is limited to  $1.1\ \mu\text{m}$ . Since the microlamp would radiate in the  $2.5\text{-}5\ \mu\text{m}$  range, it can be concluded that the photodiode cannot be used as a detector light for the optical device.

## REFERENCES

- [1] R. A. Soref, "Silicon-based optoelectronics," *Proceedings of the IEEE*, vol. 81, no. 12, pp. 1687–1706, 1993, doi: 10.1109/5.248958.
- [2] N. Tupikina, A. Kin, S. Lisakov, and E. Sypin, "Experimental testing of the complex method for increasing decision-making reliability by electro-optical device for fire detection on background of dynamic optical interferences," in *2021 IEEE 22nd International Conference of Young Professionals in Electron Devices and Materials (EDM)*, 2021, vol. 2021-June, pp. 257–264, doi: 10.1109/EDM52169.2021.9507681.
- [3] Q. Xie and J. Xu, "Recent research development of FinFETs," *Science China Physics, Mechanics & Astronomy*, vol. 59, no. 12, p. 127331, Dec. 2016, doi: 10.1007/s11433-016-0394-5.
- [4] G. M. Adema, L.-T. Hwang, G. A. Rinne, and I. Turlik, "Passivation schemes for copper/polymer thin-film interconnections used in multichip modules," *IEEE Transactions on Components, Hybrids, and Manufacturing Technology*, vol. 16, no. 1, pp. 53–59, 1993, doi: 10.1109/33.214860.
- [5] D. C. Miller, W. Zhang, and V. M. Bright, "Micromachined, flip-chip assembled, actuatable contacts for use in high density interconnection in electronics packaging," *Sensors and Actuators A: Physical*, vol. 89, no. 1–2, pp. 76–87, Mar. 2001, doi: 10.1016/S0924-4247(00)00548-3.
- [6] A. Bebee, C. J. Stubbs, and D. J. Robertson, "Large deflection model for multiple, inline, interacting cantilever beams," *Journal of Applied Mechanics*, vol. 88, no. 4, Apr. 2021, doi: 10.1115/1.4049072.
- [7] M. Buffolo *et al.*, "Degradation mechanisms of heterogeneous III-V/Silicon loop-mirror laser diodes for photonic integrated circuits," *Microelectronics Reliability*, vol. 88–90, pp. 855–858, Sep. 2018, doi: 10.1016/j.microrel.2018.06.058.
- [8] M. C. Barr *et al.*, "Direct monolithic integration of organic photovoltaic circuits on unmodified paper," *Advanced Materials*, vol. 23, no. 31, pp. 3500–3505, Aug. 2011, doi: 10.1002/adma.201101263.
- [9] J. S. Orcutt *et al.*, "Low loss waveguide integration within a thin-SOI CMOS foundry," in *2012 Optical Interconnects Conference*, 2012, pp. 25–26, doi: 10.1109/OIC.2012.6224465.
- [10] J. Li *et al.*, "Miniaturized single-fiber-based needle probe for combined imaging and sensing in deep tissue," *Optics Letters*, vol. 43, no. 8, p. 1682, Apr. 2018, doi: 10.1364/OL.43.001682.
- [11] E.-S. Lee, K.-W. Chun, J. Jin, S.-S. Lee, and M.-C. Oh, "Monolithic integration of polymer waveguide phase modulators with silicon nitride waveguides using adiabatic transition tapers," *Optics Express*, vol. 31, no. 3, p. 4760, Jan. 2023, doi: 10.1364/OE.479614.
- [12] G. T. Reed and C. E. J. Png, "Silicon optical modulators," *Materials Today*, vol. 8, no. 1, pp. 40–50, Jan. 2005, doi: 10.1016/S1369-7021(04)00678-9.
- [13] N. P. Pham, H. K. Tyagi, B. D. Bois, R. V. Hoof, and G. Winderickx, "Post processing of a SiNy-based photonic stack above a CMOS imager sensor," in *2018 IEEE 20th Electronics Packaging Technology Conference (EPTC)*, 2018, pp. 50–54, doi: 10.1109/EPTC.2018.8654381.
- [14] D. Pergande, V. Zamora, P. Lützw, and H. Heidrich, "Microring resonator arrays for sensing applications," in *Nanomaterials, Polymers, and Devices*, Wiley, 2015, pp. 291–318.
- [15] R. J. Ram, "Photonic-electronic integration with polysilicon photonics in bulk CMOS," in *Silicon Photonics X*, 2015, vol. 9367, p. 93670N, doi: 10.1117/12.2175462.
- [16] M. F. Schubert, A. K. C. Cheung, I. A. D. Williamson, A. Spyra, and D. H. Alexander, "Inverse design of photonic devices with strict foundry fabrication constraints," *ACS Photonics*, vol. 9, no. 7, pp. 2327–2336, Jul. 2022, doi: 10.1021/acsp Photonics.2c00313.

- [17] V. J. Gamero, P. H. A. Amorim, J. H. Sierra, G. P. Rehder, and M. I. Alayo, "Design and post-process of an integrated CMOS-MEMS IR emitter with an embedded detector," in *2018 SBFoton International Optics and Photonics Conference (SBFoton IOPC)*, 2018, pp. 1–5, doi: 10.1109/SBFoton-IOPC.2018.8610948.
- [18] V. J. G. Sobero, "Fabrication and characterization of an optical device developed with 0.35  $\mu\text{m}$  CMOS technology (in Portuguese)," Universidade de Sao Paulo, 2019.
- [19] J. J. P. Venter, A. L. Franc, T. Stander, and P. Ferrari, "Transmission lines characteristic impedance versus Q-factor in CMOS technology," *Int. J. Microw. Wirel. Technol.*, vol. 14, no. 4, pp. 432–437, May 2022, doi: 10.1017/S175907872100060X.
- [20] J. Tu, D. Howard, S. D. Collins, and R. L. Smith, "Micromachined, silicon filament light source for spectrophotometric microsystems," *Applied Optics*, vol. 42, no. 13, p. 2388, May 2003, doi: 10.1364/AO.42.002388.
- [21] P. GUHA *et al.*, "Novel design and characterisation of SOI CMOS micro-hotplates for high temperature gas sensors," *Sensors and Actuators B: Chemical*, vol. 127, no. 1, pp. 260–266, Oct. 2007, doi: 10.1016/j.snb.2007.07.047.
- [22] I. ShemTov *et al.*, "Design and fabrication of electrostatically formed nanowire gas sensors with integrated heaters," *Journal of Microelectromechanical Systems*, vol. 31, no. 3, pp. 442–449, Jun. 2022, doi: 10.1109/JMEMS.2022.3166212.
- [23] P. Barritault, M. Brun, S. Gidon, and S. Nicoletti, "Mid-IR source based on a free-standing microhotplate for autonomous CO2 sensing in indoor applications," *Sensors and Actuators A: Physical*, vol. 172, no. 2, pp. 379–385, Dec. 2011, doi: 10.1016/j.sna.2011.09.027.
- [24] S. Z. Ali, A. De Luca, R. Hopper, S. Boual, J. Gardner, and F. Udrea, "A low-power, low-cost infra-red emitter in CMOS technology," *IEEE Sensors Journal*, vol. 15, no. 12, pp. 6775–6782, Dec. 2015, doi: 10.1109/JSEN.2015.2464693.
- [25] K. Okamoto, *Fundamentals of Optical Waveguides*. Elsevier, 2006.
- [26] D. Pellion, K. Jradi, N. Brochard, D. Prêle, and D. Ginjac, "Single-photon avalanche diodes (SPAD) in CMOS 0.35  $\mu\text{m}$  technology," *Nuclear Instruments and Methods in Physics Research Section A: Accelerators, Spectrometers, Detectors and Associated Equipment*, vol. 787, pp. 380–385, Jul. 2015, doi: 10.1016/j.nima.2015.01.100.
- [27] B. A. Dedavid, C. I. Gomes, and G. Machado, *Scanning electron microscopy: applications and sample preparation: polymeric, metallic and semiconductor materials (in Portuguese)*. Porto Alegre: EDIPUCRS, 2007, 2007.
- [28] H. Kawasaki, T. Ohshima, Y. Yagyu, Y. Suda, S. I. Khartsev, and A. M. Grishin, "TiO<sub>2</sub>/TiN/TiO<sub>2</sub> heat mirrors by laser ablation of single TiN target," *Journal of Physics: Conference Series*, vol. 100, no. 1, p. 012038, Mar. 2008, doi: 10.1088/1742-6596/100/1/012038.

## BIOGRAPHIES OF AUTHORS



**Ricardo Yauri**    holds a master's degree in electronic engineering with a specialization in Biomedical studies. He serves as an associate professor at the Universidad Nacional Mayor de San Marcos (UNMSM) and is currently pursuing a Ph.D. in Systems Engineering. He is also a faculty member at Universidad Tecnológica del Perú and Universidad Peruana del Norte. He has actively contributed as an instructor for courses focused on the Internet of Things (IoT) and its applications in home automation, as well as being associated with the Cisco academy for IoT. His experience encompasses research work at INICTEL-UNI within the Embedded Systems and Internet of Things research group. He has undertaken research projects centered around the development of energy efficient IoT devices that incorporate inference techniques, machine learning algorithms, and computational intelligence. He can be reached at C24068@utp.edu.pe and ryaurir@unmsm.edu.pe.



**Vanessa Gamero**    is Specialist in the development of electronic systems with solid knowledge in microelectronics, digital twins and embedded firmware in electronic systems. She graduated in Electronic Engineering from the National University of Engineering. She worked at INICTEL-UNI (Peru) in the Department of Research and Technological Development. She has a Master of science degree with mention in microelectronics from the Universidade de São Paulo in Brazil. Nowadays, her research field is focus on digital well-being algorithms in her Ph.D. studies in the Universidade de Sao Paulo. She can be reached at vgamero@usp.br.



**Marco Alayo**    is Graduated in Electronic Engineering from the Universidad Privada Antenor Orrego (1993) in Trujillo-Peru. Master (1996), Doctor (2000) and post-Doctor (2004) in Electrical Engineering from the University of São Paulo (USP)-Brazil. Currently he is an Associate Professor at the Polytechnic School of the University of São Paulo. He has experience in Electrical Engineering with emphasis on optical, thermo-optical and electro-optical devices based on silicon compounds. He mainly works on the following topics: Integrated optics, optical devices and sensors, photonic crystals, micro-opto-electro-mechanical systems (MOEMS), dielectric films, PECVD and microelectronics. He can be reached at malayo@usp.br.